 CMES, vol.88, no.6, pp.443-474, 2012

Analogy Between Rotating Euler-Bernoulli and Timoshenko Beams and Stiff Strings

A.S Vinod Kumar [1] Ranjan Ganguli [2]

Abstract: The governing differential equation of a rotating beam becomes the stiff-string equation if we assume uniform tension. We find the tension in the stiff string which yields the same frequency as a rotating cantilever beam with a prescribed rotating speed and identical uniform mass and stiffness. This tension varies for different modes and are found by solving a transcendental equation using bisection method. We also find the location along the rotating beam where equivalent constant tension for the stiff string acts for a given mode. Both Euler-Bernoulli and Timoshenko beams are considered for numerical results. The results provide physical insight into relation between rotating beams and stiff string which are useful for creating basis functions for approximate methods in vibration analysis of rotating beams.

Keywords: Rotating beam, Centrifugal stiffening, Finite element, Bisection method, Frequency, Vibration.

1 Introduction

Rotating beams are often used to model blades of wind turbines [Lin, Lee and Lin (2008), Hsu (2008)], steam and gas turbines, helicopter rotors and aircraft propellers. Most vibration analysis on rotating beams seek to predict the first 3-5 frequencies accurately [Hodges and Rutkowski (1981)]. In general, the first 2-3 modes are affected by centrifugal stiffening and the higher modes are primarily governed by flexural bending. In particular, the fundamental mode shows a very strong influence of the centrifugal force which becomes very important for high speed rotating beams such as those used in turbomachinary [Gunda and Ganguli (2009)]. The centrifugal stiffening effect modifies the overall stiffness of the beam, which naturally results in the variation of natural frequencies and mode shapes.

[1] Department of Aerospace Engineering; e-mail: vinod@aero.iisc.ernet.in
[2] Corresponding author: Professor, Address: Department of Aerospace Engineering, Indian Institute of Science, Bangalore 560012, India; phone: 91-80-2293-3017; fax: 91-80-2360-0134; e-mail: ganguli@aero.iisc.ernet.in

A key feature in the mathematical model of a rotating beam is the presence of variable coefficients in the governing partial differential equation, even for a uniform beam. Since the governing differential equation for rotating beam vibration cannot be solved analytically, approximate methods such as those based on Rayleigh-Ritz and Galerkin approaches or more popularly, the finite element method, are needed to solve the rotating beam equation for the natural frequencies. An accurate approach to develop a finite element which has been used is to select accurate shape functions like hybrid stiff string based polynomials [Gunda, Gupta and Ganguli (2009)], stiff string functions [Gunda and Ganguli (2008)], higher order polynomials [Udupa and Varadan (1990)], trigonometric functions [Hashemi, Richard and Dhatt (1999)] and rational interpolation functions [Gunda and Ganguli (2008)].

Some of these basis functions satisfy the static part of the homogenous governing differential equation for the problem and ensure superior convergence rate as compared to conventional Hermite cubic elements. Some researchers have also used the dynamic stiffness method [Banerjee (2000), (2001)], Frobenius method of series solution of differential equations [Du, Kim and Liew (1994), Naguleshwaran (1994)] and differential transform method [Kaya, Özdemir (2006)] to solve for the natural frequencies of rotating beams. Spectral finite element method [Vinod, Gopalakrishnan and Ganguli(2007), Wang and Wereley (2004)] for uniform and tapered rotating beams was also developed. Yokoyama (1988) developed finite element procedure for determining free vibration characteristics of rotating Timoshenko beams. Kosmatka (1995) developed two node finite element for axially loaded Timoshenko beams.

Typically, much more progress has taken place in the development of computational methods for non-rotating beams [Lee, Lu, Liu (2008), Lai, Chen, Hsu (2008), Lee, Wu (2009)] in comparison to research on moving [Lin (2009)] and rotating beams [Lee, Lin, Lin (2009)]. Some researchers have addressed complex structures involving rotating beams with flexible roots and hubs [Al-Qaisa, (2008)]. Vadiraja and Sahasrabudhe (2008) modeled thin walled composite beams with embedded macro fibre composite actuators and sensors. Vibration control was addressed and the optimal control problem was solved using LQG control algorithm.

Despite the many research works on rotating beams, there is a need for finding analogies between these structures and simpler physical systems. The non-rotating beam is a simple system which can provide interesting analogies. For example, Ananth and Ganguli (2009) have found that a shared eigen pair exists between uniform non-rotating cantilever beams and rotating beams for a given mode. A physical structure which lies in between non-rotating beams and rotating beams in terms of mathematical complexity is the stiff string. If we assume constant tension, the governing differential equation of a rotating beam reduces to that of a stiff string i.e beam with a constant axial force. The stiff string, which is of interest in musical instruments, presents a partial differential equation which is relatively easier to solve. In this paper, we investigate the analogy between the rotating beam and the stiff string. Both Euler-Bernoulli and the Timoshenko beams are considered. The frequency equations for Euler beams with constant axial tension which was derived by Bokaian (1990) is used to match frequencies of the Euler rotating beam and to calculate equivalent centrifugal force and its location on the rotating beam. The frequency equation for non-rotating Timoshenko beam was derived by Van Rensburg and Van der Merve (2006). Using the boundary condition for beam with constant axial tension, the frequency equation for Timoshenko stiff strings is derived and equivalent axial tension required to match the rotating Timoshenko beam frequencies are calculated. The equivalent constant tensions required are calculated numerically by solving a transcendental equation using bisection method and verified using the finite element method. By equalizing tension in the stiff string to match natural frequency of the rotating beam, we have found an analogy of these two physical systems.

2 FORMULATION

2.1 Euler-Bernoulli beam

The governing equation for rotating Euler-Bernoulli beam is given by [Hodges and Rutkowski (1981)]

$$\rho A(x)\frac{\partial^2 w(x,t)}{\partial t^2} - \frac{\partial}{\partial x}(T(x)\frac{\partial w(x,t)}{\partial x}) + \frac{\partial^2}{\partial x^2}(EI(x)\frac{\partial^2 w(x,t)}{\partial x^2}) = 0 \quad (1)$$

where $T(x)$ is the axial force due to centrifugal stiffening and is given by

$$T(x) = \int_x^L \rho A(x)\Omega^2 dx \quad (2)$$

Here L is the length of beam, Ω is the rotational speed, $w(x)$ is the transverse displacement of beam, $EI(x)$ is the flexural stiffness of beam and ρ is the density of beam, as shown in Fig. 1. For a uniform beam, Eq. (1) reduces to

$$EI\frac{\partial^4 w(x,t)}{\partial x^4} + \rho A\frac{\partial^2 w(x,t)}{\partial t^2} - \frac{\partial}{\partial x}(T(x)\frac{\partial w(x,t)}{\partial x}) = 0 \quad (3)$$

If we assume $T(x) = T$ to be constant, the stiff string equation is obtained [Rossing and Fletcher (1995)]

$$EI\frac{\partial^4 w(x,t)}{\partial x^4} + \rho A\frac{\partial^2 w(x,t)}{\partial t^2} - T\frac{\partial^2 w(x,t)}{\partial x^2} = 0 \quad (4)$$

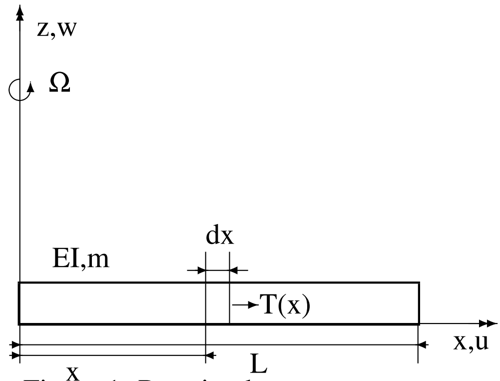

Figure 1: Rotating beam

Substituting $w(x,t)=y(x)e^{i\omega t}$ in Eq. (4) yields

$$\frac{d^4y}{dx^4} - (\frac{\rho A\omega^2}{EI})y - (\frac{T}{EI})\frac{d^2y}{dx^2} = 0 \tag{5}$$

Using transformation $\xi=\frac{x}{l}$, $\eta=\frac{y}{l}$, we get $\frac{dy}{dx}=\frac{d\eta}{d\xi}$, $\frac{d^2y}{dx^2}=\frac{1}{l}\frac{d^2\eta}{d\xi^2}$, $\frac{d^4y}{dx^4}=\frac{1}{l^3}\frac{d^4\eta}{d\xi^4}$; Eq. (5) becomes

$$\frac{d^4\eta}{d\xi^4} - (\frac{m\omega^2 l^4}{EI})\eta - (\frac{Tl^2}{EI})\frac{d^2\eta}{d\xi^2} = 0 \tag{6}$$

The roots of Eq. (6) are $\pm(\frac{Tl^2}{2EI} + \sqrt{(\frac{Tl^2}{2EI})^2 + (\frac{m\omega^2 l^4}{EI})^2})$ and $\pm(\frac{Tl^2}{2EI} - \sqrt{(\frac{Tl^2}{2EI})^2 + (\frac{m\omega^2 l^4}{EI})^2})$
Let $\eta=e^{p\xi}$, then characteristic equation for Eq. (6) is

$$p^4 - (\frac{Tl^2}{EI})p^2 - \frac{m\omega^2 l^4}{EI} = 0 \tag{7}$$

Defining non-dimensional parameters $\frac{Tl^2}{2EI}=U$(centrifugal tension), $\frac{\omega l^2}{\alpha}=\psi$(natural frequency) where $\alpha=\sqrt{\frac{EI}{\rho A}}$ we get the roots as

$$\beta = \pm(U + \sqrt{U^2 + \psi^2})^{\frac{1}{2}} \tag{8}$$

$$\gamma = \pm(U - \sqrt{U^2 + \psi^2})^{\frac{1}{2}} \tag{9}$$

The general solution for Eq. (6) is

$$\eta = c_1 \sinh(\beta\xi) + c_2 \cosh(\beta\xi) + c_3 \sin(\gamma\xi) + c_4 \cos(\gamma\xi) \tag{10}$$

We apply cantilever boundary conditions in non dimensionalized form. At $\xi = 1$

$$EI\frac{d^2\eta}{d\xi^2} = 0, EI\frac{d^3\eta}{d\xi^3} = T\frac{d^2\eta}{d\xi^2} \tag{11}$$

At $\xi = 0$

$$EI\eta = 0, EI\frac{d\eta}{d\xi} = 0 \tag{12}$$

Using Eqs. (8) and (9) and substituting for above boundary conditions and eliminating constants in Eq. (10) we get the transcendental equation for the stiff string as

$$(2U^2 + \psi^2)\cosh\beta\cos\gamma + \psi^2 + U\psi\sinh\beta\sin\gamma = 0 \tag{13}$$

Given T, EI, ρ, A, L of a stiff string or beam, we can find the natural frequency ψ by using any numerical method. By evaluating the integral in Eq. (2) for uniform beam we get

$$T = \int_x^L \rho A\Omega^2 dx = \frac{\rho A\Omega^2}{2}(L^2 - x^2) \tag{14}$$

Inserting $U = \frac{TL^2}{2EI}$, $\frac{m\Omega^2 L^4}{EI} = \kappa^2$ and $\frac{x}{L} = \mu$, we get

$$\mu = \sqrt{1 - \frac{2U}{\kappa^2}} \tag{15}$$

This is the non-dimensional location of a rotating beam where the equivalent constant tension acts.

2.2 Finite element model of Euler-Bernoulli beam

The displacement model for Euler-Bernoulli beam element with four degrees of freedom is given by

$$w = a_0 + a_1\bar{x} + a_2\bar{x}^2 + a_3\bar{x}^3 \tag{16}$$

$$\theta = \frac{dw}{d\bar{x}} = a_1 + 2a_2\bar{x} + 3a_3\bar{x}^2 \tag{17}$$

The shape functions(N_w, N_θ) are constructed by substituting for nodal degrees of freedom of element in Eq. (16) and (17). The mass and stiffness matrices can be obtained using the energy expressions. The kinetic energy($K.E$) for a Euler-Bernoulli beam is given by

$$K.E = \int_0^L \frac{1}{2}\rho[\dot{w}(x,t)^2]dx \tag{18}$$

The strain energy(U) expression is given by

$$U = \frac{1}{2}EI\int_0^L (\frac{d^2w}{dx^2})^2 dx + \frac{1}{2}\int_0^L T(x)(\frac{dw}{dx})^2 dx \tag{19}$$

Here $x_i = (i-1)l$ and $x = x_i + \bar{x}$ where l is the length of the element. The mass and stiffness matrices (M_i and K_i) for the beam element can be obtained from Eqs. (18) and (19) for a uniform beam. The calculations for these matrices involve calculating the following integrals:

$$M_i = \rho A\int_0^1 (N_w)^T(N_w)d\bar{x} \tag{20}$$

$$K_i = EI\int_0^1 (\frac{d^2N_w}{d\bar{x}^2})^T(\frac{d^2N_w}{d\bar{x}^2})(\frac{1}{l^3})d\bar{x} + \int_0^1 T_i(\bar{x})(\frac{dN_w}{d\bar{x}})^T(\frac{dN_w}{d\bar{x}})\frac{1}{l}d\bar{x} \tag{21}$$

where

$$T_i(\bar{x}) = \sum_{j=1}^{N}\int_{x_j}^{x_{j+1}} m_j(\bar{x})\Omega^2\bar{x}d\bar{x} - \int_{x_i}^{x_i+\bar{x}} m_i(\bar{x})\Omega^2\bar{x}d\bar{x} \tag{22}$$

2.3 Timoshenko beam

The governing equation for rotating Timoshenko beam is given by [Kaya (2006)]

$$\rho A(x)\frac{\partial^2 w(x,t)}{\partial t^2} - \frac{\partial}{\partial x}(T\frac{\partial w(x,t)}{\partial x}) - \frac{\partial}{\partial x}(GA(x)k(\frac{\partial w(x,t)}{\partial x} - \theta(x,t))) = 0 \tag{23}$$

$$\rho I(x)\frac{\partial^2 \theta(x,t)}{\partial t^2} + \frac{\partial}{\partial x}(EI(x)\frac{\partial \theta(x,t)}{\partial x}) - GA(x)k(\frac{\partial w(x,t)}{\partial x} - \theta(x,t)) = 0 \tag{24}$$

For uniform beam and constant tension [Kosmatka (1995)] Eqs. (23) and (24) reduce to

$$\rho A\frac{\partial^2 w}{\partial t^2} = T\frac{\partial^2 w}{\partial x^2} + GAk(\frac{\partial^2 w}{\partial x^2} - \frac{\partial \theta}{\partial x}) \tag{25}$$

$$\rho I \frac{\partial^2 \theta}{\partial t^2} = GAk(\frac{\partial w}{\partial x} - \theta) + EI\frac{\partial^2 \theta}{\partial x^2} \quad (26)$$

where θ is angle of rotation of cross section, $w(x,t)$ is the vertical displacement of beam, ρ is the density, E and G are the elastic constants, k is the shear coefficient, A is the area of cross section, I is the moment of inertia of cross section and T is the constant axial tension. We introduce non-dimensional variables as $\tau = \frac{t}{t'}$, $\xi = \frac{x}{L}$, $u(\xi,\tau)$=$\frac{w(x,t)}{L}$ and $\psi(\xi,\tau)$=$\theta(x,t)$. Here $t' = L\sqrt{\frac{\rho}{GAk}}$. The non-dimensional constants are $\alpha = \frac{AL^2}{I}$, U=$\frac{TL^2}{2EI}$, β=$\frac{GAkL^2}{EI}$ and γ=$\frac{\beta}{\alpha}$=$\frac{Gk}{E}$, $\frac{\rho A\omega^2 L^4}{EI}$=$\psi^2$. Using the same notation of physical quantities(w, θ, x, t) to denote the dimensionless quantities(u, ψ, ξ, τ), yields a system of differential equations in non-dimensional form as

$$\frac{\partial^2 w}{\partial t^2} = (1+\frac{2U}{\beta})\frac{\partial^2 w}{\partial x^2} - \frac{\partial \theta}{\partial x} \quad (27)$$

$$\frac{\partial^2 \theta}{\partial t^2} = \frac{1}{\gamma}\frac{\partial^2 \theta}{\partial x^2} - \alpha\theta + \alpha\frac{\partial w}{\partial x} \quad (28)$$

These equations can be considered to be that of a Timoshenko stiff string. Let $w(x,t) = y_1 e^{i\omega t}$, $\theta(x,t) = y_2 e^{i\omega t}$ and $\lambda = \frac{\rho A\omega^2 L^4}{EI\beta} = \frac{\psi^2}{\beta}$ then Eqs. (27) and (28) reduce to

$$-(1+\frac{2U}{\beta})\frac{d^2 y_1}{dx^2} + \frac{dy_2}{dx} = \lambda y_1 \quad (29)$$

$$-\frac{1}{\gamma}\frac{d^2 y_2}{dx^2} - \alpha\frac{dy_1}{dx} + \alpha y_2 = \lambda y_2 \quad (30)$$

Considering λ(eigenvalue) to be an arbitrary positive constant, we can derive the general solution to Eqs. (29) and (30). The function $e^{mx}\mathbf{w}$ is a solution if and only if

$$\begin{bmatrix} -m^2(1+\frac{2U}{\beta}) & m \\ -\alpha m & -\frac{1}{\gamma}m^2 + (\alpha-\lambda) \end{bmatrix} \begin{bmatrix} w_1 \\ w_2 \end{bmatrix} = \begin{bmatrix} 0 \\ 0 \end{bmatrix}$$

For nontrivial solution $\mathbf{w}$ of system, it is necessary that the determinant becomes zero,

$$m^4(1+\frac{2U}{\beta}) + m^2(\lambda(1+\gamma) - \frac{2U}{\beta}\gamma(\alpha-\lambda)) + \gamma\lambda(\lambda-\alpha) = 0 \quad (31)$$

For the roots m of characteristic equation Eq. (31) we have

$$m^2 = \frac{-1}{2(1+\frac{2U}{\beta})}(\lambda(1+\gamma) - \frac{2U}{\beta}\gamma(\alpha-\lambda)) \pm \sqrt{(\lambda(1+\gamma) - \frac{2U}{\beta}\gamma(\alpha-\lambda))^2 - a} \quad (32)$$

where $a = 4\gamma\lambda(\lambda-\alpha)(1+\frac{2U}{\beta})$ which further reduces to

$$m^2 = -\frac{\lambda(1+\gamma)}{2(1+\frac{2U}{\beta})}[1-\frac{2U}{\beta}(\frac{\alpha}{\lambda}-1)(\frac{\gamma}{1+\gamma})\pm\sqrt{(1-\frac{2U}{\beta}(\frac{\alpha}{\lambda}-1)(\frac{\gamma}{1+\gamma}))^2-G}] \quad (33)$$

where $G = 4\frac{\gamma}{(1+\gamma)^2}(1-\frac{\alpha}{\lambda})(1+\frac{2U}{\beta})$. It can be shown algebraically that for $\lambda < \alpha$, $\lambda > \alpha$ and $\lambda = \alpha$ and for given $U > 0$, $\lambda > 0$, there exists two real and two imaginary roots of form $\pm\mu$, $\pm i\nu$, four imaginary roots of form $\pm i\nu$, $\pm i\theta$ and two imaginary roots $\pm i\nu$ respectively [van Rensburg and van der Merve (2006)]. They are of form

$$\mu^2 = \frac{\lambda(1+\gamma)}{2(1+\frac{2U}{\beta})}(\Delta^{\frac{1}{2}}-\Lambda) \quad (34)$$

$$\nu^2 = \frac{\lambda(1+\gamma)}{2(1+\frac{2U}{\beta})}(\Delta^{\frac{1}{2}}+\Lambda) \quad (35)$$

$$\theta^2 = \frac{\lambda(1+\gamma)}{2(1+\frac{2U}{\beta})}(\Lambda-\Delta^{\frac{1}{2}}) \quad (36)$$

In Eqs. (34), (35) and (36)

$$\Lambda = 1-\frac{2U}{\beta}(\frac{\alpha}{\lambda}-1)(\frac{\gamma}{1+\gamma}) \quad (37)$$

$$\Delta = (1-\frac{2U}{\beta}(\frac{\alpha}{\lambda}-1)(\frac{\gamma}{1+\gamma}))^2-\frac{4\gamma(1-\frac{\alpha}{\lambda})(1+\frac{2U}{\beta})}{(1+\gamma)^2} \quad (38)$$

For case $\lambda < \alpha$. The general solution can be written as

$$\begin{bmatrix} y_1 \\ y_2 \end{bmatrix} = A\begin{bmatrix} \sinh(\mu x) \\ (\frac{\lambda+\mu^2(1+\frac{2U}{\beta})}{\mu})\cosh(\mu x) \end{bmatrix} + B\begin{bmatrix} \cosh(\mu x) \\ (\frac{\lambda+\mu^2(1+\frac{2U}{\beta})}{\mu})\sinh(\mu x) \end{bmatrix}$$
$$+C\begin{bmatrix} \sin(\nu x) \\ -(\frac{\lambda-\nu^2(1+\frac{2U}{\beta})}{\nu})\cos(\nu x) \end{bmatrix} + D\begin{bmatrix} \cos(\nu x) \\ (\frac{\lambda-\nu^2(1+\frac{2U}{\beta})}{\nu})\sin(\nu x) \end{bmatrix} \quad (39)$$

for case $\lambda = \alpha$

$$\begin{bmatrix} y_1 \\ y_2 \end{bmatrix} = A\begin{bmatrix} 0 \\ 1 \end{bmatrix} + B\begin{bmatrix} 1 \\ \alpha x \end{bmatrix} + C\begin{bmatrix} \sin(\nu x) \\ -(\frac{\lambda-\nu^2(1+\frac{2U}{\beta})}{\nu})\cos(\nu x) \end{bmatrix}$$
$$+D\begin{bmatrix} \cos(\nu x) \\ (\frac{\lambda-\nu^2(1+\frac{2U}{\beta})}{\nu})\sin(\nu x) \end{bmatrix} \quad (40)$$

for the case $\lambda > \alpha$

$$\begin{bmatrix} y_1 \\ y_2 \end{bmatrix} = A\begin{bmatrix} \sin(\theta x) \\ -\frac{(\lambda-\theta^2)}{\theta}\cos(\theta x) \end{bmatrix} + B\begin{bmatrix} \cos(\theta x) \\ \frac{\lambda-\theta^2}{\theta}\sin(\theta x) \end{bmatrix}$$
$$+C\begin{bmatrix} \sin(\nu x) \\ -(\frac{\lambda-\nu^2(1+\frac{2U}{\beta})}{\nu})\cos(\nu x) \end{bmatrix} + D\begin{bmatrix} \cos(\nu x) \\ (\frac{\lambda-\nu^2(1+\frac{2U}{\beta})}{\nu})\sin(\nu x) \end{bmatrix} \tag{41}$$

$$\text{x=0}, y_1 = 0, y_2 = 0 \tag{42}$$

$$\text{x=1}, EI\frac{dy_2}{dx} = 0, (1+\frac{2U}{\beta})\frac{dy_1}{dx} - y_2 = 0 \tag{43}$$

Applying cantilever boundary conditions for all three cases and eliminating constants yields following transcendental equation for $\lambda < \alpha$, $\lambda > 0$

$$\cosh(\mu)\cos(\nu)\left[\left(\frac{\lambda+\mu^2(1+\frac{2U}{\beta})}{\lambda-\nu^2(1+\frac{2U}{\beta})} + \frac{\lambda-\nu^2(1+\frac{2U}{\beta})}{\lambda+\mu^2(1+\frac{2U}{\beta})}\right)\right]$$
$$+(\frac{\nu}{\mu} - \frac{\mu}{\nu})\sinh(\mu)\sin(\nu) - 2 = 0 \tag{44}$$

for $\lambda > \alpha$, $\lambda > 0$

$$\cos(\theta)\cos(\nu)\left[\left(\frac{\lambda-\theta^2(1+\frac{2U}{\beta})}{\lambda-\nu^2(1+\frac{2U}{\beta})} + \frac{\lambda-\nu^2(1+\frac{2U}{\beta})}{\lambda-\theta^2(1+\frac{2U}{\beta})}\right)\right]$$
$$+(\frac{\nu}{\theta} + \frac{\theta}{\nu})\sin(\theta)\sin(\nu) - 2 = 0 \tag{45}$$

for $\lambda = \alpha$, $\lambda > 0$

$$\left(\frac{\alpha}{\alpha-\nu^2(1+\frac{2U}{\beta})} + \frac{\alpha-\nu^2(1+\frac{2U}{\beta})}{\alpha}\right)\cos(\nu) + \nu\sin(\nu) - 2 = 0 \tag{46}$$

where $\nu^2 = \frac{\lambda(1+\gamma)}{1+\frac{2U}{\beta}}$ from Eq. (35). For a given beam α, β and U are known, based on which the above equations can solved for λ using any numerical scheme which in turn gives non-dimensional natural frequencies ψ=$\sqrt{\lambda\beta}$. The location of constant tension can be found out using Eq. (15) at any given rotational speed.

2.4 Finite element model for Timoshenko beam

The displacement model for Timoshenko beam element with four degrees of freedom is given by [Reddy (1993)].

$$w = b_0 + b_1\bar{x} + a_1\frac{\bar{x}^2}{2} + a_2\frac{\bar{x}^3}{3} \tag{47}$$

$$\theta = b_1 + a_1\bar{x} + a_2(\bar{x}^2 + \frac{2EI}{GAk}) \tag{48}$$

The shape functions(N_w, N_θ) are constructed by substituting for nodal degrees of freedom of element in Eqs.(47) and (48). The mass and stiffness matrices can be obtained using the energy expressions. The kinetic energy($K.E$) for a Timoshenko beam is given by

$$K.E = \int_0^L \frac{1}{2}\rho\left[\dot{w}(x,t)^2 + \dot{u}(x,t)^2\right]dx \tag{49}$$

The strain energy(U) expression is given by

$$U = \frac{1}{2}EI\int_0^L (\frac{d\theta}{dx})^2 dx + \frac{1}{2}GAk\int_0^L (\frac{dw}{dx} - \theta)^2 dx + \frac{1}{2}T\int_0^L (\frac{dw}{dx})^2 dx. \tag{50}$$

Here $x = x_i + \bar{x}$ and $x_i = (i-1)l$, where l is length of element. The mass and stiffness matrices (M_i and K_i) for a beam element can be obtained from the energy expressions in Eqs. (49) and (50) for a uniform beam. The calculations for these matrices involve calculating the following integrals:

$$M_i = \rho A\int_0^1 (N_w)^T(N_w)\,d\bar{x} + \rho I\int_0^1 (N_\theta)^T(N_\theta)\,d\bar{x} \tag{51}$$

$$K_i = EI\int_0^1 (\frac{dN_\theta}{d\bar{x}})^T(\frac{dN_\theta}{d\bar{x}})(\frac{1}{l})\,d\bar{x} + GAk\int_0^1 (\frac{1}{l}\frac{dN_w}{d\bar{x}} - N_\theta)^T)(\frac{1}{l}\frac{dN_w}{d\bar{x}} - N_\theta)l\,d\bar{x}$$
$$+ \int_0^1 T_i(\bar{x})(\frac{dN_w}{d\bar{x}})^T(\frac{dN_w}{d\bar{x}})\frac{1}{l}\,d\bar{x} \tag{52}$$

where centrifugal tension(T_i) acting on element is given by Eq. (22)

RESULTS AND DISCUSSIONS

The results are first obtained for an Euler-Bernoulli beam and then for a Timoshenko beam.

Euler-Bernoulli beam

A finite element model is used to calculate the natural frequencies of the rotating beam at different rotation speeds. Hermite cubic elements are used to predict frequency of first five modes for Euler-Bernoulli stiff string and rotating beams. From Tab. 1, it can be seen that for $\kappa = 0$ the frequencies match with those of a non-rotating beam. At higher values of κ the natural frequencies increase because of centrifugal stiffening. These frequencies at $\kappa = 12$ and $\kappa = 100$ match with values given by [Gunda and Ganguli (2008), Hodges and Rutkowski (1981)]. As rotation speed increases, the natural frequencies increase.

Table 1: Non-dimensional frequencies(5 modes) for various values of Non-dimensional rotational parameter(κ). The results in parentheses are from [Gunda and Ganguli (2008), Hodges and Rutkowski (1981)]

κ	ψ_1	ψ_2	ψ_3	ψ_4	ψ_5
0	3.5160	22.0345	61.6972	120.9019	199.8595
	(3.5160)	(22.0345)	(61.6972)	(120.902)	(199.862)
4	5.5850	24.2733	63.9668	123.2615	202.2767
8	9.2568	29.9954	70.2930	130.0490	209.3385
10	11.2023	33.6404	74.6493	134.8841	214.4610
12	13.1702	37.6031	79.6145	140.5344	220.5363
	(13.1702)	(37.6031)	(79.6145)	(140.534)	(220.536)
20	21.1165	55.1102	103.4366	169.1921	252.5781
30	31.0949	78.4672	137.6133	212.9137	304.1643
40	41.0852	102.3635	173.6997	260.5476	362.3903
50	51.0798	126.4846	210.6379	309.9542	423.8793
70	71.0739	175.0277	285.7206	411.1330	551.2271
80	81.0722	199.3774	323.5967	462.3324	615.9627
100	101.0697	248.1585	399.7300	565.3834	746.4395

Tab. 2 shows the non-dimensional tension U required to individually match the first five modes of the stiff string with the rotating Euler-Bernoulli beam for several values of rotational speed. This tension is obtained by solving Eq. (13) using a bisection method, for natural frequency ψ obtained from the validated finite element model of the rotating beam. The bisection method is simply an application of intermediate value theorem and guarantees convergence to the root, despite having slower convergence rate compared to derivative based methods. But compared to other methods of root extraction, the bisection method has added advantage that the error is known since the roots of relevant equation are isolated in intervals. For example, at $\kappa = 12$, $U_1 = 25.2560$ is the constant tension in the string which matches the first mode frequency of stiff string with the rotating Euler-Bernoulli beam. At $\kappa = 100$, $U_1 = 2003.93$ is the constant stiff string tension required to match the first mode frequency of rotating Euler-Bernoulli beam with stiff string. It can be inferred from Tab. 2 that the value of tension required in stiff string to match the frequency of rotating beam increases as rotational speed increases. It is interesting to note that a physically analogous stiff string exists for the rotating

Table 2: Non-dimensional tension(U) required to match individually the first five mode frequencies of stiff string with rotating beam for various values of Non-dimensional rotational parameter(κ)

κ	U_1	U_2	U_3	U_4	U_5
4	2.2306	1.6122	1.8458	2.0162	2.1305
8	10.2844	6.6393	7.3722	8.0433	8.5057
10	16.9110	10.5926	11.5263	12.5502	13.2736
12	25.2560	15.6013	16.6288	18.0507	19.0888
20	75.2420	46.8833	46.9119	50.0532	52.7685
30	174.4230	111.3205	107.5294	112.6995	118.1692
40	314.1770	203.1947	193.0194	199.9768	208.8857
50	494.4751	322.1920	302.8532	311.0260	323.9221
70	976.6670	641.279	594.847	602.472	623.7975
80	1278.5610	841.3374	776.9500	782.4620	807.7346
100	2003.9300	1322.4810	1213.4500	1210.6930	1242.5605

beam over a large range of rotation speeds. From Tab. 2 for Euler-Bernoulli beam, the value of tension U required decreases upto 2^{nd} mode for values of $\kappa = 4 \ldots 20$ and increases in 3^{rd}, 4^{th} and 5^{th} mode. For values of $\kappa = 30 \ldots 80$, there is a drop in value of tension U upto 3^{rd} mode and increase in 4^{th} mode and 5^{th} mode. For $\kappa = 100$, the decrease is upto 4^{th} mode and increase in 5^{th} mode. In general, the first mode requires a high level of tension relative to the other modes which shows the importance of centrifugal stiffening on fundamental mode.

Table 3: μ v/s κ of first modes for various rotational speeds for Euler beam

κ	μ_1	μ_2	μ_3	μ_4	μ_5
4	0.6651	0.7726	0.7339	0.7042	0.6836
8	0.5977	0.7649	0.7343	0.7052	0.6844
10	0.5688	0.7591	0.7341	0.7057	0.6849
12	0.5463	0.7527	0.7335	0.7061	0.6854
20	0.4976	0.7288	0.7286	0.7067	0.6873
30	0.4741	0.7108	0.7226	0.7065	0.6891
40	0.4632	0.7014	0.7193	0.7071	0.6912
50	0.4570	0.6961	0.7179	0.7088	0.6941
70	0.4502	0.6903	0.7172	0.7129	0.7006
80	0.4482	0.6886	0.7172	0.7148	0.7037
100	0.4455	0.6863	0.7174	0.7181	0.7092

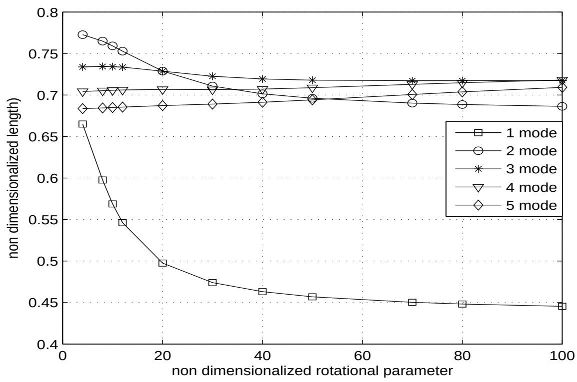

Figure 2: μ(Euler-Bernoulli) v/s κ for first five modes

Tab. 3 and Fig. 2 shows the non dimensional length along the rotating beam where the equivalent tension in the stiff string would act for a given rotation speed for the Euler-Bernoulli beam. For $\kappa = 12$, the tension corresponds to that at $\mu_1 = \frac{x}{L} = .5463$ for the first mode and moves to a maximum of .7527 for the second mode. It can be seen that while the tension U in Tab. 2 appears to be quite different for different modes and rotation speeds, the equivalent location of tension in rotating beam lies between 44 and 77 percent of beam length. From Tab. 3 we see that for first, second and third mode that there is a shift towards root for increasing values of κ. For the fourth and fifth mode, there is a slight shift towards tip for increasing values of κ. From Fig. 2 it can be seen that the first mode shows maximum change in μ and the values of μ approach a steady state at higher values of rotational speeds. Interestingly, for the higher modes, μ ranges from .65 to .8 which is relatively narrow band.

Tab. 4-Tab. 8 shows natural frequencies of first five modes of rotating Euler-Bernoulli beam obtained by putting constant tension corresponding to analogous Euler-Bernoulli stiff string for that respective mode. For example, in Tab. 4, the values of U corresponding to $\kappa = 4$ from Tab. 2 are put into the finite element analysis of Euler-Bernoulli rotating beam with tension made uniform. For $U = 2.2306$, the first frequency ψ_1 matches the finite element results. For $U = 1.6122$, the second frequency ψ_2 matches the finite element results and so on. Thus, the numerical results obtained by solving the transcendental equations are verified using finite element method.

To see the practical significance of the results in this paper, we consider the case

Table 4: Computed natural frequencies for five modes of rotating Euler-Bernoulli beam at $\kappa = 4$ for various values of corresponding constant tension in Euler-Bernoulli Stiff string

U	finite element	ψ_1	ψ_2	ψ_3	ψ_4	ψ_5
2.2306	5.5850	5.5850	5.1271	5.3069	5.4326	5.5146
1.6122	24.2733	25.0689	24.2733	24.5776	24.7967	24.9423
1.8458	63.9668	64.4295	63.6843	63.9668	64.1721	64.3095
2.0162	123.2615	123.5097	122.7924	123.0639	123.2615	123.3939
2.1305	202.2767	202.3895	201.6913	201.9554	202.1477	202.2767

Table 5: $\kappa = 8$

U	finite element	ψ_1	ψ_2	ψ_3	ψ_4	ψ_5
10.2844	9.2568	9.2568	7.9011	8.1993	8.4594	8.6323
6.6393	29.9954	33.3754	29.9954	30.7157	31.3559	31.7868
7.3722	70.2930	73.3789	69.4911	70.2930	71.0181	71.5127
8.0433	130.0490	132.4776	128.5020	129.3120	130.0490	130.5541
8.5057	209.3305	211.2649	207.2970	208.1012	208.8347	209.3386

Table 6: $\kappa = 12$

U	finite element	ψ_1	ψ_2	ψ_3	ψ_4	ψ_5
25.256	13.1702	13.1702	10.8530	11.1282	11.4955	11.7548
15.6013	37.6031	43.9749	37.6031	38.3489	39.3501	40.0601
16.6288	79.6145	87.2360	78.6453	79.6145	80.9322	81.8778
18.0507	140.5344	147.5636	138.0507	139.0988	140.5345	141.5721
19.0888	220.5363	226.7858	216.9149	217.9887	219.4652	220.5363

Table 7: $\kappa = 80$

U	finite element	ψ_1	ψ_2	ψ_3	ψ_4	ψ_5
1278.5610	81.0722	81.0722	66.0910	63.5798	63.7987	64.79298
841.3374	199.3774	244.1185	199.3774	191.8869	192.5399	195.5050
776.9500	323.5967	409.8514	335.9417	323.5968	324.6725	329.5583
782.4620	462.3324	580.0004	477.8564	460.8516	462.3325	469.0610
807.7346	615.9627	756.2099	627.0440	605.6273	607.4912	615.9628

where one finite element is used to obtain the rotating beam frequencies. The classical approach is to use polynomials such as $w(x) = a_0 + a_1 x + a_2 x^2 + a_3 x^3$. This cubic equation represents the solution of $EI\frac{d^4 w}{dx^4} = 0$ which is the static homoge-

Table 8: $\kappa = 100$

U	finite element	ψ_1	ψ_2	ψ_3	ψ_4	ψ_5
2003.9300	101.0697	101.0697	82.4238	79.0251	78.9372	79.9469
1322.4810	248.1585	303.9333	248.1586	238.0003	237.7377	240.7553
1213.4500	399.7300	508.9592	416.5368	399.7302	399.2959	404.2872
1210.6930	565.3834	717.5577	589.2622	565.9849	565.3836	572.2945
1242.5605	746.4395	931.0395	767.9572	738.4429	737.6809	746.4399

nous differential equation for a non-rotating beam. Applying beam finite element conditions at the nodes, the displacement is written in terms of Hermite basis functions, $w(x) = H_1q_1 + H_2q_2 + H_3q_3 + H_4q_4$ where $H_1 = 1 - \frac{3x^2}{l^2}$, $H_2 = \frac{x}{l} - \frac{2x^2}{l^2} + \frac{x^3}{l^3}$, $H_3 = \frac{3x^2}{l^2} - \frac{2x^3}{l^3}$, $H_4 = \frac{x^3}{l^3} - \frac{x^2}{l^2}$ are the Hermite basis functions and q_i are the degrees of freedom($i = 1 \ldots 4$) at the nodes. The static homogenous differential equation for a rotating beam from Eq. (3) as, $EI\frac{d^4w}{dx^4} - \frac{d}{dx}(T(x)\frac{dw}{dx}) = 0$. The presence of $T(x)$ in this equation presents a problem in obtaining an exact solution. Considering $T(x) = T$, leads to an exact solution for the stiff string of the form $w(x)$=a_0+a_1x+a_2e^{-ax}
+a_3e^{ax}. The corresponding basis functions are $H_1 = \frac{N_1}{D}, H_2 = \frac{N_2}{CD}, H_3 = \frac{N_3}{D}, H_4 = \frac{N_4}{CD}$
Here

$$N_1 = -(-e^{Cl} - e^{-Cl} + 2 + lCe^{Cl} - lCe^{-Cl} - Cxe^{Cl} + Cxe^{-Cl} - e^{-C(x-l)} + e^{-Cx} - e^{C(x-l)} + e^{Cx})$$

$$N_2 = -lCe^{Cl} - lCe^{-Cl} + e^{Cl} - e^{-Cl} - 2Cx + Cxe^{Cl} + Cxe^{-Cl} + e^{-Cx+Cl}lC - e^{-Cx+Cl} + e^{-Cx} + e^{Cx-Cl}lC + e^{Cx-Cl} - e^{Cx}$$

$$N_3 = -2 + e^{Cl} + e^{-Cl} - Cxe^{Cl} + Cxe^{-Cl} - e^{-Cx+Cl} + e^{-Cx} - e^{Cx-Cl} + e^{Cx}$$

$$N_4 = -e^{Cl} + e^{-Cl} + 2Cl - 2Cx + Cxe^{Cl} + Cxe^{-Cl} + e^{-Cx+Cl} - e^{-Cx}lC - e^{-Cx} - e^{Cx-Cl} - e^{Cx}lC + e^{Cx}$$

where

$$D = -4 - lCe^{Cl} + lCe^{-Cl} + 2e^{Cl} + 2e^{-Cl} \text{ and } C = \sqrt{\frac{T}{EI}}$$

We now use the value of T corresponding to the first mode and compute stiff string basis function. Tab. 9 gives converged values of fundamental frequency at $\kappa = 12$, 40 and 100 respectively along with one element results using cubic and stiff string basis functions. The present basis function shows better convergence of fundamental mode compared to cubic, especially at high rotation speeds as they capture centrifugal effects well.

Table 9: Comparison of fundamental frequency of rotating Euler-Bernoulli beam($\kappa = 12, 40$ and 100), obtained using one element by placing equivalent centrifugal tension at fundamental mode location(μ_1)

κ	converged FEM	cubic	stiff string(μ_1)
12	13.1702	13.5392	13.1741
40	41.0852	43.1812	41.0902
100	101.0697	111.8802	101.0752

Table 10: Non-dimensional frequencies(5 modes) for various values of Non-dimensional rotational parameter(κ). The results in parentheses are from [Du, Lim and Liew (1994)] for $\alpha = 123.4568$, $\gamma = .25$.

κ	ψ_1	ψ_2	ψ_3	ψ_4	ψ_5
0	3.2303(3.230)	14.5415	31.6716	48.5358	64.2781
4	5.2495(5.249)	17.2564	35.3418	52.8709	67.5575
8	8.7444(8.744)	23.4149	43.8097	61.2022	73.8592
10	10.6002	26.9971	48.6674	64.343	78.4682
12	12.4872(12.487)	30.6897	53.4932	66.564	83.2667
20	20.1841	44.7861	67.9999	73.4151	95.3483
30	29.9144	56.0802	75.5078	85.6088	102.9718
40	39.6054	60.463	77.8861	102.9584	107.2329
50	49.0283	62.6245	78.9200	105.1857	128.2295
70	61.0048	71.7479	79.9869	105.9933	136.2178
80	62.1624	79.0717	82.0386	106.1894	136.3684
100	62.9977	80.21	100.6873	106.4597	136.5608

Timoshenko beam

The Timoshenko beam is sensitive to choice of slenderness ratio. Several slenderness ratios are considered for he numerical results. The non-dimensional beam properties used for the Timoshenko beam are slenderness ratio $\frac{r}{L}$ = .09, .05, .045, cross section shape factor $k = \frac{2}{3}$, $\frac{E}{G} = \frac{8}{3}$ [Du, Lim and Liew (1994)]. A finite element model is used to obtain the frequencies of rotating Timoshenko beam. Here we use field consistent interpolation displacement model as given in Eqs. (47) and (48) to determine shape functions and determine stiffness and mass matrices for the Timoshenko stiff string(App. B) and rotating beam. From Tab. 10, it can be seen that for $\kappa = 0$ the frequencies match with those of a non-rotating beam. These results are obtained for a slenderness ratio of .09 and a cross section shape factor of $\frac{2}{3}$. At higher values of κ, the natural frequencies increase because of centrifugal stiffening. These frequencies at κ = 0, 4, 8 and 12 match with values given by [Du, Lim and Liew (1994)]. As expected, the relative rise in natural frequencies is highest for the first mode.

Table 11: Non-dimensional tension(U) required to match individually the first five mode frequencies of stiff string with rotating beam for various values of Non-dimensional rotational parameter(κ)

κ	U_1	U_2	U_3	U_4	U_5
4	2.4449	1.8961	2.2821	2.4423	2.6926
8	11.2891	7.6637	8.7121	9.4464	10.2009
10	18.327	11.998	13.2798	14.9994	15.3255
12	27.043	17.2412	18.6882	22.1234	22.427
20	78.218	45.4997	61.6056	48.956	52.3472
30	178.212	86.889	105.6787	147.6974	68.5391
40	317.288	130.872	121.06	254.88	160.424
50	492.24	213.645	139.605	324.775	348.6821
70	814.855	1024.366	226.7	442.54	434.73
80	888.77	1330.16	1223.960	516.15	499.24
100	1011.7	1532.85	2030.913	732.57	721.4

Tab. 11 shows the non-dimensional tension U required to individually match the first five modes of the Timoshenko stiff string with the rotating Timoshenko beam for several values of rotational speed. Here, U is found for Eqs. (44)-(46) using bisection method for a natural frequency ψ obtained from finite element model. The eigenvalue λ for corresponding ψ is obtained and substituted in Eqs. (44)-(46)

Table 12: μ v/s κ of first modes for various rotational speeds for Timoshenko beam

κ	μ_1	μ_2	μ_3	μ_4	μ_5
4	0.6235	0.7252	0.6553	0.6240	0.5717
8	0.5426	0.7218	0.6749	0.6400	0.6020
10	0.5166	0.7212	0.6847	0.6325	0.6221
12	0.4988	0.7219	0.6935	0.6209	0.6140
20	0.4667	0.7382	0.6196	0.7145	0.6903
30	0.4560	0.7835	0.7282	0.5861	0.8339
40	0.4547	0.8203	0.8351	0.6023	0.7739
50	0.4609	0.8113	0.8813	0.6931	0.6649
70	0.5786	0.4047	0.9027	0.7992	0.8032
80	0.6667	0.4107	0.4848	0.8230	0.8294
100	0.7716	0.6220	0.4332	0.8408	0.8435

and root extraction is done for different isolated intervals. For example, at $\kappa = 12$, $U_1 = 27.043$, is the constant tension in the string which matches the first mode frequency of Timoshenko stiff string with rotating Timoshenko beam. At $\kappa = 100$, $U_1 = 1011.7$ is the constant stiff string tension required to match the first mode frequency of rotating Timoshenko with stiff string. It can be inferred from Tab. 11 that the value of tension required in stiff string to match the frequency of rotating beam increases as rotational speed increases. From Tab. 11 for Timoshenko beam, there is a drop in value of tension upto 2^{nd} mode for values of $\kappa = 4\ldots30$ and increase in 3^{rd}, 4^{th} and 5^{th} modes. For values of $\kappa = 40\ldots70$, there is drop in value of tension upto 3^{rd} mode and increase in 4^{th} mode. For $\kappa = 80$, there is an increase upto 2^{nd} mode followed by decrease in 3^{rd}, 4^{th} and 5^{th} modes, while that for $\kappa = 100$ the increase is upto 3^{rd} mode followed by decrease in 4^{th} and 5^{th} mode. It shows that for a given rotating beam operating at a given rotation speed, there exists an analogous Timoshenko stiff string which has the same frequency for a given mode. For $\kappa = 4\ldots50$ the tension is highest for first mode, for $\kappa = 70$ and 80 it is highest for 2^{nd} mode, while for $\kappa = 100$ the maximum tension occurs for 3^{rd} mode.

Tab. 12 and Fig. 3 shows the non dimensional length along rotating beam where the equivalent tension in stiff string would act for a given rotation speed for Timoshenko beam. For $\kappa = 12$, the tension corresponds to that at $\mu_1 = \frac{x}{L} = .4988$ for the first mode and moves to a maximum of .7219 for the second mode. It can be seen that equivalent location of tension in rotating beam lies between 45 and 90 percent of beam length. From Tab. 12 we see that for 1^{st} mode that there is a shift towards root for values of $\kappa = 4\ldots40$ and shifts towards tip at $\kappa = 50\ldots100$. At values of $\kappa = 30\ldots100$ there is a shift towards tip for 4^{th} mode and for the 5^{th} mode there is

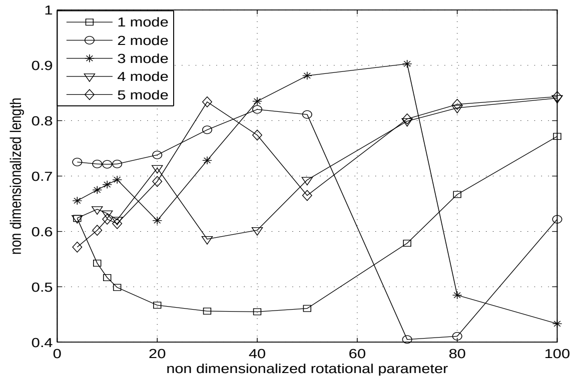

Figure 3: μ(Timoshenko) v/s κ for first five modes for slenderness ratio $\frac{r}{L} = .09$

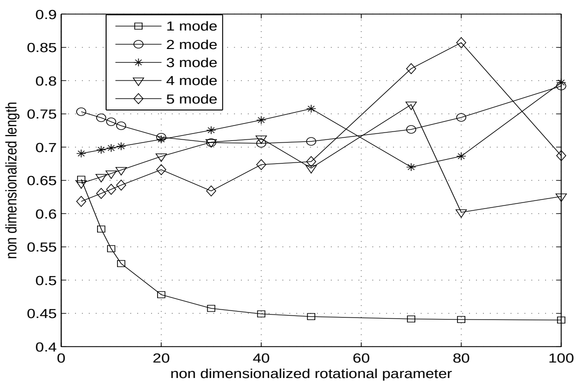

Figure 4: μ(Timoshenko) v/s κ for first five modes for for slenderness ratio $\frac{r}{L} = .05$

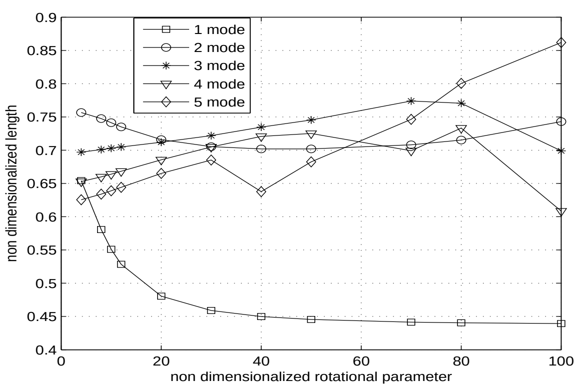

Figure 5: μ(Timoshenko) v/s κ for first five modes for slenderness ratio $\frac{r}{L} = .045$

Table 13: Computed natural frequencies for five modes of rotating Timoshenko beam at $\kappa = 4$ for various values of corresponding constant tension in Timoshenko Stiff string

U	finite element	ψ_1	ψ_2	ψ_3	ψ_4	ψ_5
2.4449	5.2495	5.2495	4.9036	5.1507	5.2480	5.3947
1.8961	17.2564	17.9543	17.2568	17.7508	17.9511	18.2587
2.2821	35.3418	35.5897	34.7538	35.3441	35.5858	35.9596
2.4423	52.8709	52.8808	51.9723	52.6152	52.8765	53.2783
2.6926	67.5575	67.3241	66.7591	67.1618	67.3216	67.5637

Table 14: $\kappa = 8$

U	finite element	ψ_1	ψ_2	ψ_3	ψ_4	ψ_5
11.2891	8.7444	8.7444	7.5733	7.9343	8.1753	8.4140
7.6637	23.4149	26.4509	23.4154	24.3397	24.9629	25.5846
8.7121	43.8097	46.6494	42.5786	43.8121	44.6478	45.4834
9.4464	61.2022	62.4924	59.6406	60.6027	61.2058	61.7696
10.2009	73.8592	74.8481	71.6764	72.5604	73.1975	73.8657

Table 15: $\kappa = 12$

U	finite element	ψ_1	ψ_2	ψ_3	ψ_4	ψ_5
27.043	12.4872	12.4872	10.3386	10.6857	11.4637	11.5297
17.2412	30.6897	36.4341	30.6903	31.6198	33.7033	33.8799
18.6882	53.4932	59.2099	52.2945	53.4956	56.0951	56.3080
22.1234	66.5640	67.7997	65.1617	65.6168	66.5657	66.6440
22.4270	83.2667	85.2297	80.0367	81.0911	83.1204	83.2715

appreciable shift towards tip for all values of κ except at $\kappa = 30$ and 50. For 2^{nd} and 3^{rd} modes the shift varies differently for various values of κ. Fig. 4 and Fig. 5 shows variation of μ for slenderness ratios of .05 and .045. It can be seen that their variation approach that of Euler-Bernoulli stiff string given in Fig. 2 as the slenderness ratio decreases. The Timoshenko stiff string analogy presents a complicated behavior in the location of effective equivalent tension relative to Euler-Bernoulli beam.

Tab. 13-Tab. 17 shows natural frequencies of first five modes of rotating Timoshenko beam obtained by putting constant tension corresponding to Timoshenko stiff string for that respective mode using finite element method assuming uniform tension. Again, the numerical results obtained using the finite element method val-

Table 16: $\kappa = 80$

U	finite element	ψ_1	ψ_2	ψ_3	ψ_4	ψ_5
888.77	62.1624	62.1633	63.5788	63.4700	50.1592	49.3630
1330.16	79.0717	67.8915	79.0776	77.2105	64.1177	64.0667
1223.96	82.0386	81.0595	83.3958	82.0468	80.7006	80.6807
516.15	106.1894	106.5725	106.7126	106.6882	106.2018	106.1648
499.24	136.3684	136.6660	136.7688	136.7506	136.4191	136.3946

Table 17: $\kappa = 100$

U	finite element	ψ_1	ψ_2	ψ_3	ψ_4	ψ_5
1011.7	62.9977	62.9988	63.7076	63.8597	58.8196	58.4585
1532.85	80.2100	71.3734	80.2212	80.6504	65.1813	65.0826
2030.913	100.6873	81.2298	88.1100	100.6883	80.9084	80.8985
732.57	106.4597	106.6248	106.7511	106.8398	106.4758	106.4669
721.4	136.5608	136.7035	136.7974	136.8474	136.5984	136.5928

Table 18: Comparison of fundamental frequency of rotating Timoshenko beam($\kappa = 12, 40$ and 100), obtained using one element by placing equivalent centrifugal tension at fundamental mode location(μ_1) for slenderness ratio of $\alpha = 123.4568$

κ	Converged FEM	cubic	stiff string(μ_1)
12	12.4872	13.0508	12.4935
40	39.6054	39.8753	39.8022
100	62.9977	64.2730	85.6011

Table 19: Comparison of fundamental frequency of rotating Timoshenko beam($\kappa = 12, 40$ and 100), obtained using one element by placing equivalent centrifugal tension at fundamental mode location(μ_1) for slenderness ratio of $\alpha = 400$

κ	Converged FEM	cubic	stiff string(μ_1)
12	12.8274	15.3140	13.6482
40	40.2189	44.5521	44.1025
100	99.7241	109.9721	109.8621

idate the results obtained by solving the transcendental equation using bisection method.

The consistent interpolation field using cubic polynomial for Timoshenko beam is given in Eqs. (47) and (48). This equation represents the solution of $GAk(\frac{\partial^2 w}{\partial x^2} - \frac{\partial \theta}{\partial x}) = 0$, $GAk(\frac{\partial w}{\partial x} - \theta) + EI\frac{\partial^2 \theta}{\partial x^2} = 0$ which is the static homogenous equation for a

Table 20: Comparison of fundamental frequency of rotating Timoshenko beam($\kappa = 12, 40$ and 100), obtained using one element by placing equivalent centrifugal tension at fundamental mode location(μ_1) for slenderness ratio of $\alpha = 493.82716$

κ	Converged FEM	cubic	stiff string(μ_1)
12	12.8750	15.8227	13.6665
40	40.2792	44.7433	44.1419
100	99.8493	110.1948	109.9694

non-rotating Timoshenko beam. Applying beam finite element conditions at nodes, the displacement and rotation is written in terms of basis functions, $w(x) = H_{w1}q_1 + H_{w2}q_2 + H_{w3}q_3 + H_{w4}q_4$ and $\theta(x) = H_{\theta 1}q_1 + H_{\theta 2}q_2 + H_{\theta 3}q_3 + H_{\theta 4}q_4$ where H_{wi} and $H_{\theta i}$ are displacement and rotation shape functions($i = 1 \dots 4$) which are derived in App. B. The static homogenous differential equation for Timoshenko rotating beam are Eqs. (23) and (24). As the presence of $T(x)$ in the equations presents a problem, consider $T(x) = T$ which leads to exact solution of form $w(x) = a_0 + a_1x + a_2e^{-ax} + a_3e^{ax}$, $\theta(x) = b_0 + b_1e^{-ax} + b_2e^{ax}$. Here $a = \sqrt{\frac{T}{EI(1+\frac{T}{GAk})}}$. The corresponding basis functions are derived in App. A.

Tab. 18 shows convergence of fundamental mode using Timoshenko stiff string and cubic basis functions for one element at $\kappa = 12$ and 40 and 100 at slenderness ratio of $\alpha = 123.4568$. It can be seen that Timoshenko stiff string exhibits better convergence than cubic for the first mode. But at higher rotational speeds they tend to become less effective because Timoshenko effects are predominant.

From Tab. 19 and Tab. 20 shows convergence of fundamental mode at slenderness ratios of $\alpha = 400$ and 493.82716. It can be seen that as the slenderness ratio increases i.e as the beam approaches Euler-Bernoulli the centrifugal effects are more predominant for the fundamental mode at higher rotational speeds than the rotary and shear deformation effects. Hence as this mode is more effected due to centrifugal effect, it is effectively captured at higher rotational speeds using Timoshenko stiff string in the limit of Euler-Bernoulli. Thus the behavior of the Timoshenko beam is quite different from the Euler-Bernoulli beam especially for predicting fundamental mode at higher rotational speeds.

3 Conclusions

An analogy between rotating beams and a stiff string is found in this paper for uniform Euler-Bernoulli and Timoshenko beams. The stiff string equations are obtained by assuming uniform tension in the rotating beam equation and represent a physical system which is midway in the level of complexity between the non-rotating beam and the rotating beam. The tension in the stiff string which yields the same frequency as a rotating beam for a given mode is found. The tension rises for higher modes but equivalent location of tension along the beam length varies between 44 and 77 percent for the Euler-Bernoulli beam. For Timoshenko beam, the variation is between 40 to 90 percent. The Euler-Bernoulli beam shows a large variation in the equivalent tension location of the first mode while the Timoshenko beam shows that the effect is spread over all the modes considered. The Timoshenko beam results approach the Euler-Bernoulli results as beam becomes more slender. The new basis functions for rotating Euler-Bernoulli and Timoshenko beams using stiff string analogy shows better convergence for first mode than normally used cubic.

References

Al-Qaisia, A. A. (2008): Dynamics of a rotating beam with flexible root and flexible hub. *Structural Engineering and Mechanics*, vol. 30, no. 4, pp. 427-444.

Banerjee, J. R. (2001): Dynamics stiffness formulation and free vibration analysis of centrifugally stiffened Timoshenko beams. *Journal of Sound and Vibration*, vol. 247, no. 1, pp. 97-115.

Banerjee, J. R. (2000): Free vibration of Centrifugally stiffened uniform and tapered beams using the Dynamic Stiffness Method. *Journal of Sound and Vibration*, vol. 233, no. 5, pp. 857-875.

Bokaian, A. (1990): Natural frequencies of beams under tensile loads. *Journal of Sound and Vibration*, vol. 142, no. 3, pp. 481-498.

van Rensburg, N. F. J.; van der Merve, A. J. (2006): Natural frequencies and modes of a Timoshenko Beam. *Wave Motion*, vol. 44, no. 1, pp. 58-69.

Cook, R. D; Malkus, D. S.; Plesha, M. E.; Witt, R. J. (2002): *Concepts and Applications of Finite Element Analysis*, New York, John Wiley and Sons.

Du, H.; Lim, M. K.; Liew, K. M. (1994): A power series solution for vibration of a rotating Timoshenko Beam. *Journal of Sound and Vibration*, vol. 175, no. 4, pp. 505-523.

Gunda, J. B.; Ganguli, R. (2009): Hybrid Stiff string Basis Functions for Vibration Analysis of High Speed Rotating Beams. *Computers and Structures*, vol. 87, no. 2, pp. 254-256.

Gunda, J. B.; Ganguli, R. (2008a): Stiff string Basis Functions for Vibration Analysis of High Speed Rotating Beams. *Journal of Applied Mechanics*, vol. 75, no. 2, pp. 0245021-0245025.

Gunda, J. B.; Ganguli, R. (2008b): New Rational Interpolation Functions for Finite Element Analysis of High Speed Rotating Beams. *International Journal of Mechanical Sciences*, vol. 50, no. 3, pp. 578-588.

Hashemi, S. M.; Richard, M. J.; Dhatt, G. A. (1999): New Dynamic Finite Element Formulation for Free Lateral Vibrations of Euler-Bernoulli Spinning Beams using Trigonometric Shape Functions. *Journal of Sound and Vibration*, vol. 220, no. 4, pp. 601-624.

Hodges, D. H.; Rutkowski, M. J. (1981): Free-vibration Analysis of Rotating Beams by a Variable-order Finite Element Method. *AIAA Journal*, vol. 19, no. 11, pp. 1459-1466.

Kaya, M. O. (2006): Free vibration analysis of a rotating Timoshenko beam by differential transform method. *Aircraft Engineering and Aerospace Technology*, vol. 78, no. 3, pp. 194-203.

Kosmatka, J. B. (1995):An Improved two-node finite element for stability and natural frequencies of axially loaded Timoshenko beams. *Computers and Structures*, vol. 57, no. 1, pp. 141-149.

Kumar, A.; Ganguli, R. (2009): Rotating Beams and Non-Rotating Beams with Shared Eigenpair. *ASME Journal of Applied Mechanics*, vol. 76, no. 5, pp. 1-14.

Lai, H. Y.; Chen, C. K.; Hsu, J. C. (2008): Free Vibration of Non-Uniform Euler-Bernoulli Beams by the Adomian Modified Decomposition Method. *Computer Modeling in Engineering and Sciences*, vol. 34, no. 1, pp. 87-115.

Lee, S. Y.; Wu, J. S. (2009): Exact Solutions for the Free Vibration of Extensional Curved Non-uniform Timoshenko Beams. *CMES: Computer Modeling in Engineering and Sciences*, vol. 40, no. 2, pp. 133-154.

Lee, S. Y.; Lu, S. Y.; Liu, Y. R. (2008): Exact Large Deflection Solutions for Timoshenko Beams with Non-Linear Boundary Conditions. *CMES: Computer Modeling in Engineering and Sciences*, vol. 33, no. 3, pp. 293-312.

Lin, S. M. (2009): Vibration supression of a moving beam subjected to an active-control electrostatic force. *CMES: Computer Modeling in Engineering and Sciences*, vol. 43, no. 3, pp. 73-90.

Lin, S. M.; Lin, Y. S.; Lee, S. Y. (2009): Instability and vibration of a rotating Timoshenko beam with precone. *CMES: Computer Modeling in Engineering and Sciences*, vol. 51, no. 2, pp. 114-121.

Lin, S. M.; Lee, S. Y.; Lin, Y. S. (2008): Modeling and bending vibration of the blade of a horizontal-axis wind power turbine. *CMES: Computer Modeling in Engineering and Sciences*, vol. 23, no. 3, pp. 175-186.

Naguleswaran, N. (1994): Lateral vibration of a Centrifugally Tensioned Uniform Euler- Bernoulli Beam. *Journal of Sound and Vibration*, vol. 176, no. 5, pp. 613-624.

Özdemir, Ö.; Kaya, M. O. (2006): Flapwise bending vibration analysis of a rotating tapered cantilevered Euler Bernoulli beam by differential transform method. *Journal of Sound and Vibration*, vol. 289, no. 4, pp. 413-420.

Reddy, J. N. (2003): *An Introduction to the Finite Element Method* 2nd edition New York, McGraw-Hill.

Hildebrand, F. B. (1965): *Methods of Applied Mathematics*, Prentice City Hall.

Rossing, T. D; Fletcher, N. H. (1995): *Principles of Vibration and Sound*, New York, Springer-Verlag.

Udupa, K. M.; Varadan, T. K. (1990): Hierarchical finite element method for rotating beams. *Journal of Sound and Vibration*, vol. 138, no. 3, pp. 447-456.

Vadiraja, D. N.; Sahasrabudhe, A. D. (2008): Vibration and control of rotating tapered thin-walled composite beam using macro fiber composite actuator. *CMES: Computer Modeling in Engineering and Sciences*, vol. 27, no. 1-2, pp. 49-62.

Vinod, K. G.; Gopalakrishnan, S.; Ganguli, R. (2007): Free vibration and wave propagation analysis of uniform and tapered rotating beams using spectrally formulated finite elements. *International Journal of Solids and Structures*, vol. 44, no. 1, pp. 194-203.

Wang, G.; Wereley, N. M. (2004): Free vibration analysis of rotating blades with uniform tapers. *AIAA Journal*, vol. 42, no. 12, pp. 2429-2437.

Yokoyama, T. (1988): Free vibration characteristics of rotating Timoshenko beams. *International Journal of Mechanical Sciences*, vol. 30, no. 10, pp. 734-755.

Appendix A: Timoshenko Stiff string basis functions

The homogenous governing equation involving constant tension for a Timoshenko beam is given in Eqs .(25) and (26). After dropping the inertia term and eliminating coupling between them, the equations become

$$EI\frac{\partial^3\theta}{\partial x^3} - \left(\frac{T}{1+\frac{T}{GAk}}\right)\theta = 0 \qquad (53)$$

$$EI\frac{\partial^4 w}{\partial x^4} - \left(\frac{T}{1+\frac{T}{GAk}}\right)w = 0 \qquad (54)$$

The solutions are

$$\theta = b_0 + b_1 e^{-dx} + b_2 e^{dx} \qquad (55)$$

where $d=\sqrt{\frac{T}{EI(1+\frac{T}{GAk})}}=\sqrt{\frac{C^2}{(1+C^2m_3)}}$ and $C=\sqrt{\frac{T}{EI}}, m_3=\frac{EI}{GAk}$. Using Eqs. (53), (25) and (26), the displacement field is derived in terms of rotation shape functions given by

$$\begin{aligned} w &= b_0x+b_1\frac{e^{-dx}}{(1+C^2m_3)}((\frac{-1}{d})-\alpha x(1+C^2m_3)) \\ &\quad +b_2\frac{e^{dx}}{(1+C^2m_3)}((\frac{1}{d})-\alpha x(1+C^2m_3))+a_0\frac{1}{(1+C^2m_3)} \end{aligned} \tag{56}$$

Applying finite element boundary conditions at nodes for the element of length l and eliminating constants give interpolation fields for displacements and rotations.

$$\begin{bmatrix} w_1 \\ \theta_1 \\ w_2 \\ \theta_2 \end{bmatrix} = \begin{bmatrix} 0 & \frac{-1}{d(1+C^2m_3)} & \frac{1}{d(1+C^2m_3)} & \frac{1}{(1+C^2m_3)} \\ 1 & 1 & 1 & 0 \\ l & \frac{e^{-dl}(\frac{-1}{d}-\alpha l(1+C^2m_3))}{(1+C^2m_3)} & \frac{e^{dl}(\frac{1}{d}-\alpha l(1+C^2m_3))}{(1+C^2m_3)} & \frac{1}{(1+C^2m_3)} \\ 1 & e^{-dl} & e^{dl} & 0 \end{bmatrix} \begin{bmatrix} b_0 \\ b_1 \\ b_2 \\ a_0 \end{bmatrix}$$

The displacement and rotation field in terms of nodal degrees of freedom are given by

$$w=\begin{bmatrix} x & \frac{e^{-dx}(\frac{-1}{d}-\alpha x(1+C^2m_3))}{(1+C^2m_3)} & \frac{e^{dx}(\frac{1}{d}-\alpha x(1+C^2m_3))}{(1+C^2m_3)} & \frac{1}{(1+C^2m_3)} \end{bmatrix} c_1^{-1} \begin{bmatrix} w_1 \\ \theta_1 \\ w_2 \\ \theta_2 \end{bmatrix} \tag{57}$$

$$\theta=\begin{bmatrix} 1 & e^{-dx} & e^{dx} & 0 \end{bmatrix} c_1^{-1} \begin{bmatrix} w_1 \\ \theta_1 \\ w_2 \\ \theta_2 \end{bmatrix} \tag{58}$$

where

$$c_1=\begin{bmatrix} 0 & \frac{-1}{d(1+C^2m_3)} & \frac{1}{d(1+C^2m_3)} & \frac{1}{(1+C^2m_3)} \\ 1 & 1 & 1 & 0 \\ l & \frac{e^{-dl}(\frac{-1}{d}-\alpha l(1+C^2m_3))}{(1+C^2m_3)} & \frac{e^{dl}(\frac{1}{d}-\alpha l(1+C^2m_3))}{(1+C^2m_3)} & \frac{1}{(1+C^2m_3)} \\ 1 & e^{-dl} & e^{dl} & 0 \end{bmatrix} \textit{and}$$

$$\alpha=m_3d^2+\frac{1}{(1+C^2m_3)}-1$$

Eqs. (57) and (58) simplifies to

$$w(x) = N_{w1}w_1 + N_{w2}w_2 + N_{w3}w_3 + N_{w4}w_4 \tag{59}$$

$$\theta(x) = N_{\theta 1}\theta_1 + N_{\theta 2}\theta_2 + N_{\theta 3}\theta_3 + N_{\theta 4}\theta_4 \tag{60}$$

where

$$H_{w1} = \frac{N_1}{D}, H_{w2} = \frac{N_2}{dD}, H_{w3} = \frac{N_3}{D}, H_{w4} = \frac{N_4}{dD}$$

Here

$$\begin{aligned}
&N_1 = 2 + e^{dl}\alpha ld + e^{-dx} - e^{-dl} - e^{-dl}\alpha ld - dxe^{dl}C^2m_3 \\
&+e^{d(-l+x)}\alpha xdC^2m_3 - e^{-d(-l+x)} + e^{dx} - e^{-dl}\alpha ldC^2m_3+ \\
&e^{-dx}\alpha xd + e^{dl}\alpha ldC^2m_3 - dxe^{dl} + dxe^{-dl} - e^{-d(-l+x)}\alpha xdC^2m_3 \\
&+dxe^{-dl}C^2m_3 + e^{-dx}\alpha \\
&xdC^2m_3 - e^{dx}\alpha xdC^2m_3 - e^{dl} - e^{d(-l+x)}+ \\
&e^{dl}ld + e^{dl}ldC^2m_3 - e^{-dl}ld - e^{dx}\alpha \\
&xd - e^{-dl}ldC^2m_3 + e^{d(-l+x)}\alpha xd \\
&-e^{-d(-l+x)}\alpha xd
\end{aligned}$$

$$\begin{aligned}
&N_2 = (1 + C^2m_3)(-e^{d(-l+x)}\alpha ldC^2m_3 - e^{d(-l+x)}ld + e^{dl}\alpha ld \\
&-e^{-dx} + 2dxC^2m_3 + e^{-dl} + e^{-dl}\alpha ld - e^{d(-l+x)}\alpha ld+ \\
&2e^{d(-l+x)}\alpha^2xd^2lC^2m_3 - e^{-d(-l+x)}ld - e^{-d(-l+x)}ldC^2m_3 \\
&-2e^{-d(-l+x)}\alpha xd^2lC^2m_3 - dxe^{dl}C^2m_3 + e^{d(-l+x)}\alpha xdC^2m_3- \\
&e^{-d(-l+x)}\alpha xd^2C^4m_3^2l - e^{d(-l+x)}ldC^2m_3 + 2e^{d(-l+x)}\alpha xd^2lC^2m_3 \\
&-e^{-d(-l+x)}\alpha^2xd^2l + e^{-d(-l+x)} + e^{dx} + e^{-dl}\alpha ldC^2m_3 - e^{-dx}\alpha xd+ \\
&e^{dl}\alpha ldC^2m_3 - dxe^{dl} - dxe^{-dl} + e^{-d(-l+x)}\alpha xdC^2m_3 \\
&-e^{-d(-l+x)}\alpha^2xd^2C^4m_3^2l + e^{d(-l+x)}\alpha xd^2l - e^{-d(-l+x)}\alpha ldC^2m_3+ \\
&e^{d(-l+x)}\alpha xd^2C^4m_3^2l - e^{-d(-l+x)}\alpha ld - dxe^{-dl}C^2m_3 \\
&-e^{-dx}\alpha xdC^2m_3 - e^{dx}\alpha xdC^2m_3 - e^{dl} - e^{d(-l+x)} + 2dx + e^{dl}ld + e^{dl}ldC^2m_3+ \\
&e^{-dl}ld - 2e^{-d(-l+x)}\alpha^2xd^2lC^2m_3 - e^{-d(-l+x)}\alpha xd^2l - e^{dx}\alpha xd \\
&+e^{-dl}ldC^2m_3 + e^{d(-l+x)}\alpha^2xd^2C^4m_3^2l + e^{d(-l+x)}\alpha^2xd^2l + e^{d(-l+x)}\alpha xd+ \\
&e^{-d(-l+x)}\alpha xd)
\end{aligned}$$

$$\begin{aligned}
&N_3 = dxe^{dl} + dxe^{dl}C^2m_3 - dxe^{-dl} - dxe^{-dl}C^2m_3 - e^{-dx} + e^{-dx+dl} \\
&-e^{-dx}\alpha xd + e^{-dx+dl}\alpha xd - e^{-dx}\alpha xdC^2m_3 + e^{-dx+dl}\alpha xdC^2m_3 \\
&+e^{dx-dl} - e^{dx} - e^{dx-dl}\alpha xd + e^{dx}\alpha xd - e^{dx-dl}\alpha xdC^2m_3 \\
&+e^{dx}\alpha xdC^2m_3 - e^{dl} + 2 - e^{-dl}
\end{aligned}$$

$$N_4 = (1+C^2m_3)(-e^{dx}\alpha xd^2l - e^{dl}\alpha ld + e^{-dx} - 2dl - 2ldC^2m_3 + 2dxC^2m_3 + e^{dx-dl}\alpha ld - e^{-dl} - e^{-dl}\alpha ld + e^{dx-dl}\alpha ldC^2m_3 + e^{-dx+dl}\alpha ldC^2m_3 - dxe^{dl}C^2m_3 - e^{-dx+dl} - 2e^{dx-dl}\alpha^2xd^2lC^2m_3 - e^{dx} + e^{-dx+dl}\alpha^2xd^2l - e^{-dl}\alpha ldC^2m_3 + e^{dx-dl} - e^{dx-dl}\alpha xd + e^{-dx}\alpha xd + e^{-dx+dl}\alpha^2xd^2C^4m_3^2l - e^{dl}\alpha ldC^2m_3 - dxe^{dl} - dxe^{-dl} + e^{dx}ld + e^{-dx}ld - e^{dx-dl}\alpha xdC^2m_3 - e^{-dx+dl}\alpha xd - 2\alpha xd^2e^{-dl}lC^2m_3 - \alpha xd^2C^4m_3^2e^{-dl}l + e^{dx}ldC^2m_3 - 2e^{dx}\alpha xd^2lC^2m_3 - e^{dx}\alpha xd^2C^4m_3^2l + e^{-dx}ldC^2m_3 + e^{-dx}\alpha xd^2l + e^{-dx}\alpha xd^2C^4m_3^2l + 2e^{-dx}\alpha xd^2lC^2m_3 - e^{-dx+dl}\alpha xdC^3m_3 - dxe^{-dl}C^2m_3 - dxe^{-dl}C^2m_3 + e^{-dx}\alpha xdC^2m_3 + e^{dx}\alpha xdC^2m_3 + e^{dl} + 2e^{-dx+dl}\alpha^2xd^2lC^2m_3 - e^{dx-dl}\alpha^2xd^2l + 2dx - e^{dx-dl}\alpha^2xd^2C^4m_3^2l + \alpha xd^2C^4m_3^2e^{dl}l + \alpha xd^2e^{dl}l + 2\alpha xd^2e^{dl}lC^2m_3 - \alpha xd^2e^{-dl}l + e^{-dx+dl}\alpha ld + e^{dx}\alpha xd)$$

where

$$D = -2e^{dl} + 4 - 2e^{-dl} + e^{dl}ld + e^{dl}ldC^2m_3 - e^{-dl}ld - e^{-dl}ldC^2m_3 + e^{dl}\alpha ld + e^{dl}\alpha ldC^2m_3 - e^{-dl}\alpha ld - e^{-dl}\alpha ldC^2m_3.$$

Appendix B: Derivation of Stiffness and Mass Matrix for Timoshenko beam element with constant axial force

Let the length of element be l and L be the length of beam. From strong form of governing equation for Timoshenko beam we have

$$GAk(\frac{\partial^2 w}{\partial x^2} - \frac{\partial \theta}{\partial x}) = 0 \tag{61}$$

$$GAk(\frac{\partial w}{\partial x} - \theta) + EI\frac{\partial^2 \theta}{\partial x^2} = 0 \tag{62}$$

Eliminating w in above equations yields $EI\frac{\partial^3\theta}{\partial x^3} = 0$ for which the solution is of form

$$\theta = a_0 + a_1x + a_2x^2 \tag{63}$$

This solution is substitued in Eq. (61) and solved for w which yields

$$w = a_1\frac{x^2}{2} + a_2\frac{x^3}{3} + a_3x + a_4 \tag{64}$$

There are five independent constants for above solution but only four boundary conditions for finite element model. We subsitute Eqs. (63) and (64) in Eq. (61) we get $a_0 = a_3 + \frac{2EI}{GAk}$ which when substituted in Eq. (63) gives

$$\theta = a_3 + a_1x + a_2(x^2 + \frac{2EI}{GAk}) \tag{65}$$

and

$$w = a_4 + a_3 x + a_1 \frac{x^2}{2} + a_2 \frac{x^3}{3} \tag{66}$$

Replacing a_3 with b_1 and a_4 with b_0 we get Eqs. (47) and (48). Using this displacement model for Timoshenko beam, we substitute for nodal degrees of freedom as given by

$$w_1(\bar{x} = 0) = b_0 \tag{67}$$

$$\theta_1(\bar{x} = 0) = \frac{1}{l}\left(b_1 + 2a_2 \frac{EI}{GAk}\right) \tag{68}$$

$$w_2(\bar{x} = 1) = b_0 + b_1 + \frac{1}{2}a_1 + \frac{1}{3}a_2 \tag{69}$$

$$\theta_2(\bar{x} = 1) = \frac{1}{l}\left(b_1 + a_1 + a_2 + 2a_2 \frac{EI}{GAk}\right) \tag{70}$$

Writing Eq. (47) and (48) in matrix form we get

$$w = \begin{bmatrix} 1 & \bar{x} & \frac{\bar{x}^2}{2} & \frac{\bar{x}^3}{3} \end{bmatrix} \begin{bmatrix} b_0 \\ b_1 \\ a_1 \\ a_2 \end{bmatrix}$$

$$\theta = \begin{bmatrix} 0 & 1 & \bar{x} & \bar{x}^2 + \frac{2EI}{GAk} \end{bmatrix} \begin{bmatrix} b_0 \\ b_1 \\ a_1 \\ a_2 \end{bmatrix}$$

$$\begin{bmatrix} w_1 \\ \theta_1 \\ w_2 \\ \theta_2 \end{bmatrix} = \begin{bmatrix} 1 & 0 & 0 & 0 \\ 0 & \frac{1}{l} & 0 & \frac{2}{l}\frac{EI}{GAk} \\ 1 & 1 & 1/2 & 1/3 \\ 0 & \frac{1}{l} & \frac{1}{l} & \frac{1}{l}(1 + \frac{2EI}{GAk}) \end{bmatrix} \begin{bmatrix} b_0 \\ b_1 \\ a_1 \\ a_2 \end{bmatrix}$$

Eliminating constants b_0, b_1, a_1, a_2 we can write displacement model in terms of nodal degrees of freedom as

$$w = \begin{bmatrix} 1 & \bar{x} & \frac{\bar{x}^2}{2} & \frac{\bar{x}^3}{3} \end{bmatrix} \begin{bmatrix} 1 & 0 & 0 & 0 \\ 0 & \frac{1}{l} & 0 & \frac{2}{l}\frac{EI}{GAk} \\ 1 & 1 & 1/2 & 1/3 \\ 0 & \frac{1}{l} & \frac{1}{l} & \frac{1}{l}(1 + \frac{2EI}{GAk}) \end{bmatrix}^{-1} \begin{bmatrix} w_1 \\ \theta_1 \\ w_2 \\ \theta_2 \end{bmatrix}$$

$$\theta = \begin{bmatrix} 0 & 1 & \bar{x} & \bar{x}^2 + \frac{2EI}{GAk} \end{bmatrix} \begin{bmatrix} 1 & 0 & 0 & 0 \\ 0 & \frac{1}{l} & 0 & \frac{2}{l}\frac{EI}{GAk} \\ 1 & 1 & 1/2 & 1/3 \\ 0 & \frac{1}{l} & \frac{1}{l} & \frac{1}{l}(1 + \frac{2EI}{GAk}) \end{bmatrix}^{-1} \begin{bmatrix} w_1 \\ \theta_1 \\ w_2 \\ \theta_2 \end{bmatrix}$$

which upon simplification reduces to

$$w = \begin{bmatrix} \frac{1+12m_3-12\bar{x}m_3-3\bar{x}^2+2\bar{x}^3}{1+12m_3} \\ \frac{\bar{x}l(1+6m_3-2\bar{x}-6xm_3+\bar{x}^2)}{1+12m_3} \\ \frac{-\bar{x}(-12m_3-3\bar{x}+2\bar{x}^2)}{1+12m_3} \\ \frac{\bar{x}l(-6m_3-\bar{x}+6m_3+\bar{x}^2)}{1+12m_3} \end{bmatrix} \begin{bmatrix} w_1 \\ \theta_1 \\ w_2 \\ \theta_2 \end{bmatrix}$$

$$\theta = \begin{bmatrix} \frac{6\bar{x}(-1+\bar{x})}{1+12m_3} \\ \frac{l(1+12m_3-4\bar{x}-12\bar{x}m_3+3\bar{x}^2)}{1+12m_3} \\ \frac{-6\bar{x}(-1+\bar{x})}{1+12m_3} \\ \frac{l\bar{x}(-2+12m_3+3\bar{x})}{1+12m_3} \end{bmatrix} \begin{bmatrix} w_1 \\ \theta_1 \\ w_2 \\ \theta_2 \end{bmatrix}$$

The stiffness matrix is given by

$$K_i = \begin{bmatrix} a_{11} & a_{12} & a_{13} & a_{14} \\ a_{21} & a_{22} & a_{23} & a_{24} \\ a_{31} & a_{32} & a_{33} & a_{34} \\ a_{41} & a_{42} & a_{43} & a_{44} \end{bmatrix} \text{ where}$$

$$a_{11} = \frac{12m_2}{l(12m_3+1)^2} + \frac{2Um_2(\frac{1}{5l(12m_3+1)^2} + \frac{1}{l})}{L^2} + \frac{6m_2(l^2 - 20lm_3 - 2l + 120m_3^2 + 20m_3 + 1)}{5lm_3(12m_3+1)^2}$$

$$a_{12} = a_{21} = \frac{6m_2}{(12m_3+1)^2} + \frac{72lm_2m_3^2 + \frac{m_2(60l-60l^2)m_3}{10} + \frac{m_2(l^2-2l+1)}{10}}{m_3(12m_3+1)^2} + \frac{Um_2}{5L^2(12m_3+1)^2}$$

$$a_{13} = a_{31} = -\frac{12m_2}{l(12m_3+1)^2} - \frac{2Um_2(\frac{1}{5l(12m_3+1)^2} + \frac{1}{l})}{L^2} - \frac{6m_2(l^2 - 20lm_3 - 2l + 120m_3^2 + 20m_3 + 1)}{5lm_3(12m_3+1)^2}$$

$$a_{14} = a_{41} = \frac{6m_2}{(12m_3+1)^2} + \frac{72lm_2m_3^2 + \frac{m_2(60l-60l^2)m_3}{10} + m_2(l^2-2l+1)10}{m_3(12m_3+1)^2} + \frac{Um_2}{5L^2(12m_3+1)^2}$$

$$a_{22} = lm_2 + \frac{3lm_2}{(12m_3+1)^2} + \frac{2Um_2(\frac{l}{12} + \frac{l}{20(12m_3+1)^2})}{L^2} + \frac{2lm_2(360l^2m3^2 + 15l^2m_3 + l^2 - 180lm_3^2 - 30lm_3 - 2l + 90m_3^2 + 15m_3 + 1)}{15m_3(12m_3+1)^2}$$

$$a_{23} = a_{32} = -\frac{6m_2}{(12m_3+1)^2} + \frac{-72lm_2m_3^2 - \frac{m_2(60l-60l^2)m_3}{10} - \frac{m_2(l^2-2l+1)}{10}}{m_3(12m_3+1)^2} - \frac{Um_2}{5L^2(12m_3+1)^2}$$

$$a_{24} = a_{42} = \frac{3lm_2}{(12m_3+1)^2} - \frac{-\frac{lm_2(720l^2+720l-360)m_3^2}{30} + \frac{lm_2(60l^2-120l+60)m_3}{30} + \frac{lm_2(l^2-2l+1)}{30}}{m_3(12m_3+1)^2} - lm_2 - \frac{2Um_2(\frac{l}{12} - \frac{1}{20(12m_3+1)^2})}{L^2}$$

$$a_{33} = \frac{12m_2}{l(12m_3+1)^2} + \frac{2Um_2(\frac{1}{5l(12m_3+1)^2} + \frac{1}{l})}{L^2} + \frac{6m_2(l^2 - 20lm_3 - 2l + 120m_3^2 + 20m_3 + 1)}{5lm_3(12m_3+1)^2}$$

$$a_{34} = a_{43} = -\frac{6m_2}{(12m_3+1)^2} + \frac{-72lm_2m_3^2 - \frac{m_2(60l-60l^2)m_3}{10} - \frac{m_2(l^2-2l+1)}{10}}{m_3(12m_3+1)^2} - \frac{Um_2}{5L^2(12m_3+1)^2}$$

$$a_{44} = lm_2 + \frac{\frac{2lm_2(360l^2-180l+90)m_3^2}{15} + \frac{2lm_2(15l^2-30l+15)m_3}{15} + \frac{2lm2(l^2-2l+1)}{15}}{m_3(12m_3+1)^2} + \frac{3lm_2}{(12m_3+1)^2} + \frac{2Um_2(\frac{l}{12} + \frac{l}{20(12m_3+1)^2})}{L^2}$$

The mass matrix is given by

$$M_i = \begin{bmatrix} b_{11} & b_{12} & b_{13} & b_{14} \\ b_{21} & b_{22} & b_{23} & b_{24} \\ b_{31} & b_{32} & b_{33} & b_{34} \\ b_{41} & b_{42} & b_{43} & b_{44} \end{bmatrix}$$

where

$$b_{11} = \frac{6lm_4}{5(12m_3+1)^2} + \frac{lm_{11}(1680m_3^2+294m_3+13)}{35(12m_3+1)^2}$$

$$b_{12} = b_{21} = \frac{l^2m_{11}(1260m_3^2+231m_3+11)}{210(12m_3+1)^2} - \frac{l^2m_4(60m_3-1)}{10(12m_3+1)^2}$$

$$b_{13} = b_{31} = \frac{3lm_{11}(560m_3^2+84m_3+3)}{70(12m_3+1)^2} - \frac{6lm_4}{5(12m_3+1)^2}$$

$$b_{14} = b_{41} = -\frac{l^2m_4(60m_3-1)}{10(12m_3+1)^2} - \frac{l^2m_{11}(2520m_3^2+378m_3+13)}{420(12m_3+1)^2}$$

$$b_{22} = \frac{l^3m_{11}}{120} + \frac{l^3m_{11}}{840(12m_3+1)^2} + \frac{2l^3m_4(360m_3^2+15m_3+1)}{15(12m_3+1)^2}$$

$$b_{23} = b_{32} = \frac{l^2m_4(60m_3-1)}{10(12m_3+1)^2} + \frac{l^2m_{11}(2520m_3^2+378m_3+13)}{42(12m_3+1)^2}$$

$$b_{24} = b_{42} = \frac{l^3m_{11}}{840(12m_3+1)^2} - \frac{l^3m_{11}}{120} - \frac{l^3m_4(-720m_3^2+60m_3+1)}{30(12m_3+1)^2}$$

$$b_{33} = \frac{6m_4}{5(12m_3+1)^2} + \frac{lm_{11}(1680m_3^2+294m_3+13)}{35(12m_3+1)^2}$$

$$b_{34} = b_{43} = \frac{l^2m_4(60m_3-1)}{10(12m_3+1)^2} - \frac{l^2m_{11}(1260m_3^2+231m_3+11)}{210(12m_3+1)^2}$$

$$b_{44} = \frac{l^3m_{11}}{120} + \frac{l^3m_{11}}{840(12m_3+1)^2} + \frac{2l^3m_4(360m_3^2+15m_3+1)}{15(12m_3+1)^2}$$

where $m_2 = EI, m_3 = \frac{EI}{GAk}, m_4 = \rho I, m_{11} = \rho A, U = \frac{TL^2}{2EI}$.